Turk J Phys
29 (2005) , 17 – 24.

Determination of Defect Distribution in a Ga-rich ZnO/CdS/Cu(In,Ga)Se_2 Solar Cell by Admittance Spectroscopy

Habibe BAYHAN
Department of Physics, Muğla University, 48000 Muğla-TURKEY
e-mail: hbayhan@mu.edu.tr

Received 14.10.2003

Abstract

This article presents a study on the energy distribution of defects in efficient thin film ZnO/CdS/ Cu(In,Ga)Se_2 heterojunction solar cell by the use of admittance spectroscopy. The capacitance spectra of the device has been analyzed using a model based on the existence of a homogeneous distribution of bulk acceptors in the absorber Cu(In,Ga)Se_2 layer. This model reveals an emission from a distribution of hole traps centered at an activation energy of about 300 meV with a defect density of 1.2×10^{17} eV^{-1} cm^{-3}. The band gap of the absorber layer is estimated to be about 1.46 eV which corresponds to a Ga content of about $x \approx 0.7$ with x the ratio Ga/(Ga+In).

Key Words: CIGS, solar cell, admittance spectroscopy, defect distribution.

1. Introduction

Thin film polycrystalline solar cells based on Cu(In,Ga)Se_2 (CIGS) chalcopyrite alloys as an absorber material, a CdS buffer layer and a ZnO window layer are of considerable interest, for their potential to be among the most efficient solar producers of solar power generation [1, 2] with excellent outdoor stability [3], low cost [4] and radiation hardness [5]. As previously shown [6–10], the electrical behavior and the performances of chalcopyrite thin film solar cells are influenced mainly by impurity levels in the bulk of the space charge region and at the interface of the heterojunction. Thus, the characterization of these defect states is a clearly important step for further improvements of CIGS-based heterostructures. Towards this need, admittance spectroscopy (AS) has emerged as a powerful tool for the investigation of bulk and surface defects in these solar cells [8, 11, 12]. AS of Cu(In,Ga)Se_2-based heterojunction solar cells mostly shows two electronic transitions, known as N_1 and N_2. The transition N_1 is associated to dangling bonds due to surface anion (Se) vacancies and involves spatially discrete distribution of interface donors [8]. It has typical activation energies between 50 and 200 meV [13]. N_2 type transitions indicate a homogeneous distribution of bulk acceptors ($\sim$280$-$300 meV) [14, 15]. Since, the occupation of trapping levels locating in the vicinity of the electron (hole) quasi Fermi level E_F^n (E_F^p) changes with the application of ac signal, the contribution of the traps to the junction capacitance can be evaluated from the frequency and temperature dependent capacitance spectra $C(T, f)$.

This paper is organized as follows. After briefly describing the preparation method for the cells and the experimental setup, a short overview on the theoretical background of admittance spectroscopy is given.

Then, results on the energy distribution of defect states in the band gap of the Cu(In,Ga)Se_2 layer studied by the complex admittance of the ZnO/CdS/Cu(In,Ga)Se_2 heterojunction is presented. Additionally, we also include an analysis based on the normal incidence optical transmittance spectra taken from the layers grown on plain glass substrates, in an attempt to determine the optical band gap hence the Ga content of the absorber layer.

2. Experimental Details

Al:ZnO/CdS/Cu(In,Ga)Se_2/Mo/Glass solar cells of area 0.5 cm^2 were prepared in the Institüt für Physikalische Electronic (IPE) at the University of Stuttgart. The 2 μm Cu(In,Ga)Se_2 thin layer was deposited by coevaporation of Cu, In, Ga and Se onto Mo-coated soda-lime glass substrates. CdS buffer layer of about 0.01 μm thick was deposited by chemical bath deposition and the window ZnO layer (≈500 nm) was deposited by RF sputtering technique. The device structure was completed by the evaporation of Al metal grid onto the ZnO layer. Details of the fabrication steps are described elsewhere [16]. The carrier concentrations of n and p regions of the typical solar cell are on the order of 10^{16} cm^{-3} and 10^{18} cm^{-3}, respectively, so that the device structure can readily be represented as n^+p. The typical efficiencies of the investigated devices are between 11% –12% .

The admittance measurements were carried out at zero dc bias using a Hewlett Packard HP 4192A impedance analyzer operating at frequencies ranging from 100 Hz to 1 MHz. For the measurements, a standard device was mounted in an evacuated Oxford Instruments closed-cycle helium cryostat equipped with a sample holder which was heated in the temperature range of 100–330 K. The amplitude of the ac signal was held at 50 mV. The admittance data were evaluated assuming a parallel equivalent circuit.

The band gap of CIGS thin layers deposited onto cleaned glass substrates were determined using optical transmission at normal incidence obtained using a Perkin Elmer Lambda 19 UV/VIS/NIR spectrophotometer. The spectra were taken with reference to air at room temperature.

3. Basic Theoretical Principles of the Admittance Spectroscopy

Admittance spectroscopy is a technique which involves the measurement of admittance, i.e., capacitance C and conductance G of a rectifying junction as a function of frequency f and temperature T. The complex admittance is defined as

$$Y(\omega) = G(\omega) + i\omega C(\omega) \tag{1}$$

Since the real and imaginary part of $Y(\omega)$ are related by the Kramers-Kronig relations [17], both $G(\omega, T)$ and $C(\omega, T)$spectrums contains completely the same information. For a n^+p heterojunction device containing only shallow donors and acceptors, the depletion layer capacitance can simply be given as

$$C_{dep} = \frac{\varepsilon_s}{w} = \left(\frac{\varepsilon_s\, q\, N_A}{2\, V_{bi}}\right), \tag{2}$$

where w is the width of the depletion region, V_{bi} is the built-in voltage, ε_s is the dielectric constant of the semiconductor, N_A is the acceptor concentration and q is the elementary charge. The response of majority carriers at a measurement frequency f is limited by the dielectric relaxation time [18],

$$\tau_{rel} = \frac{\varepsilon_s}{\sigma}, \tag{3}$$

where σ is the conductivity. When angular modulation frequency $\omega = 2\pi f$ exceeds τ_{rel}^{-1}, the majority carriers can not respond to the measurement frequency. In the presence of electronically active traps in the depletion region of this device structure, the occupation of trapping levels located in the vicinity of the electron (hole) quasi Fermi level E_F^n (E_F^p) changes with the application of an ac signal. The additional contribution of a single majority trap level to the junction capacitance is [19]

$$C = C_{geo}(\omega) + \frac{C_{lf} - C_{DR}}{1 + \omega^2 \tau^{*^2}}, \tag{4}$$

where C_{lf} is the low frequency capacitance and depends on the trap density N_T and N_A in case of p-type material. τ^* is the time constant and depends on N_A, N_T and w [19]. If $N_T << N_A$, the time constant approximates the value $\tau^* = 1/\omega_o$, where ω_o is the inflection frequency of the electronic transition and corresponds to minima of $\omega\frac{dC}{d\omega}$ versus ω variation [14]. It can be simply defined as [11, 13]

$$\omega_o(T) = 2\, N_V v_{th} \sigma_p \exp(-E_a/kT) = \xi_o T^2 \exp(-E_a/kT), \tag{5}$$

where σ_p represents the capture cross section for holes, v_{th} is the thermal velocity, N_V is the effective density of states in the valence band and E_a is the activation energy of the defect with respect to the corresponding band edge. All the temperature independent parameters are included in the emission factor ξ_o.

The model proposed by Walter et al. [14] yields a clear visualization for energetically continuous and spatially homogeneous distribution of traps from the analysis of the capacitance spectra of a heterojunction device having small trap densities $N_T < N_A$. When the angular frequency of ac signal is smaller than the inflection frequency ($\omega << \omega_o$), the occupation of the trap level can follow the applied ac signal. Hence, the trap level contributes to the total capacitance. This additional capacitance can be written as a function of the applied ac signal as,

$$C_{Trap} \propto \frac{\omega_o^2(T)}{(\omega_o^2(T) + \omega^2)}. \tag{6}$$

In this model, the influence of continuous trap distribution to the capacitance is computed essentially through the approximation of eq. (6) by a step function and integration over energy and space. In addition, the contributions of all states to the capacitance originating from exchange of free carriers with the band edges were assumed to be sufficiently fast. Then the distribution of defects in energy $N_T(E)$ is expressed as

$$N_T(E_\omega) = c(E_\omega)\frac{\omega}{kT}\frac{dC(\omega)}{d\omega} = \frac{c(E_\omega)}{kT}\frac{dC(\omega)}{d\ln\omega}, \tag{7}$$

where $c\,(E_\omega)$ denotes the contribution of defects which depends on their energetic depth and on the band diagram of the heterojunction. The expression given by eq. (5) is used to convert the frequency axis into an energy axis, as

$$E_\omega = E_a(\omega) = k\,T\,\ln(2\xi_o T^2\,/\omega). \tag{8}$$

The activation energy of such N2 transitions is equal to the energy distance $E_{a2} = E_A - E_V$, where E_A denotes the energy of bulk acceptor traps as shown in Figure 1. An energetically continuous but locally discrete interface trap states also produce a step in the $C(\omega, T)$ spectrum [13]. The activation energies of these N1 states are calculated from inflection frequencies of the spectrum by taking the derivative of the capacitance spectra with respect to frequency. In this case, the thermal activation energy ω_o of depends on the bias dependent position of E_F^n or E_F^p at the junction interface. Thus, the activation energy of such transitions corresponds to the energetic difference between the Fermi energy and the conduction band energy ($E_{a1} = E_C - E_F$) at the interface (see Figure 1).

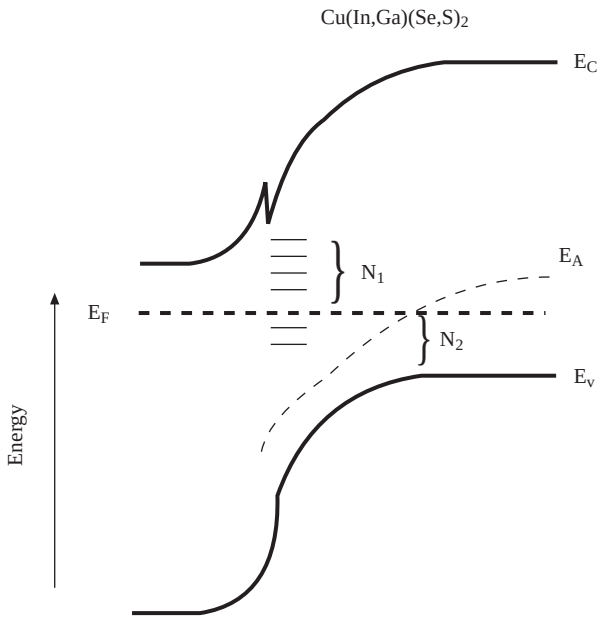

Figure 1. Schematic equilibrium band diagram of the CdS/Cu(In,Ga)(Se,S)$_2$heterojunction. Here, E_C, E_V, and E_F denote the conduction band, valence band and Fermi energy, respectively [8].

4. Results and Discussions

4.1. Admittance spectroscopy

Typical capacitance spectra measured in the frequency range between 100 Hz and 1 MHz and in the temperature range between 100 K and 320 K in steps of 10 K are shown in Figure 2. Between 100−180 K, the capacitance changes only slightly in the whole frequency range. The value for the capacitance at 100 K and 1 MHz is attributed to the depletion region capacitance. A total depletion layer width of $w \approx$1.20 μm is calculated according to eq. (2) with the assumption $\varepsilon_s = 10\varepsilon_o$, where ε_o is the vacuum permittivity. This value can not be attributed to the thickness of the CIGS layer, because it is about 2μm. In general, for all the cases of the CIGS devices, the turn-on conditions (transition between the depletion layer capacitance and the geometric capacitance) occur at 1 MHz frequency between 70 K and 10 K [11]. Due to the type of inversion usually found at the CdS/CIGS interface or to the CIGS doping, the minimum departure of the Fermi level position from the delocalized band edges across the device is always small enough to give a turn-on in the temperature range investigated.

A capacitance step observed above 200 K is attributed to the release of trapped charges. In order to analyze this step, the derivative of the capacitance spectra with respect to frequency is calculated. The inflection frequency ω_o for the trap level as a function of temperature is determined from the minima position of the frequency in a plot of fdC/df versus f (not shown here). Both the activation energy E_a and the emission factor ξ_o of a main defect contribution are determined as 293 meV and 3.2×10^6 s^{-1}K^{-2}, respectively from the Arrhenius plot presented in Figure 3.

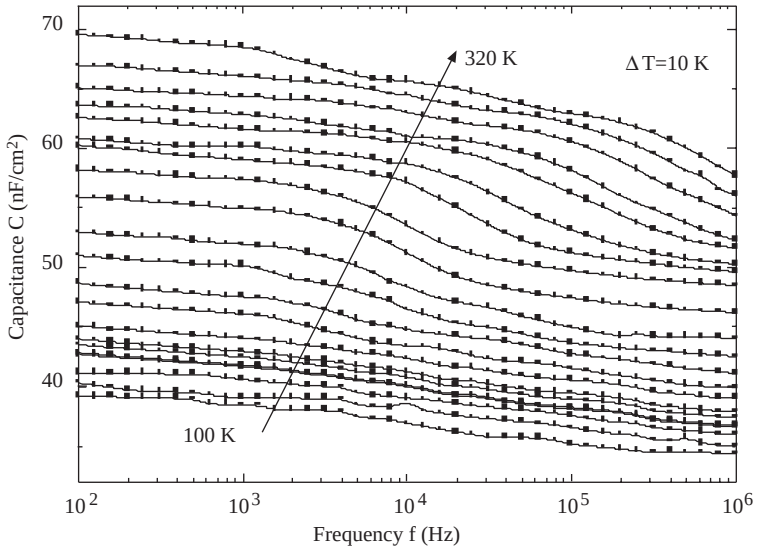

Figure 2. Capacitance spectra $C(f)$ of a typical Cu(In,Ga)Se_2 solar cell.

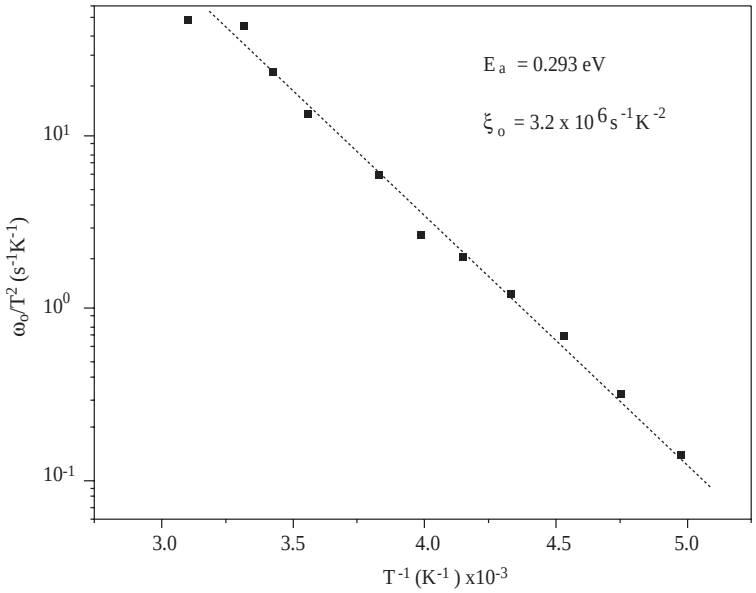

Figure 3. Arrhenius plot of the inflection frequencies determined from the derivative dC/df.

To visualize the energetic distribution of defect densities N_T over E_a, first the frequency axis is converted into an energy axis according to eq. (8) by using the extracted value for ξ_o. Then N_T (E_a) is calculated from the differentiated capacitance spectra given by eq. (7). Finally, all N_T versus E_a data evaluated at temperatures between 200 K and 320 K are superimposed and illustrated in Figure 4. This plot displays a peak centered at a defect density $1.2{\times}10^{17}$ eV^{-1} cm^{-3} with an activation energy of about 300 meV. This is in good agreement with the energy value determined from Figure 3. This transition (N2) is usually related to an emission from a distribution of hole traps in the bulk or at the grain boundaries of the Cu(In,Ga)Se_2 absorber layer [9]. In general, the study of CIGS based solar cells prepared under similar conditions, suggested that the N2 level behaves as a major recombination center and its concentration has an important effect on the efficiency of these devices [7]. The density of this defect is not only a function of stiochiometry [20] but also varies with the Ga-content in the CIGS absorber with the highest concentration ($N_T \geq 2{\times}10^{17}$ eV^{-1} cm^{-3}) in pure $CuGaSe_2$[7, 21]. This may suggests that the Ga content of the device is about $x > 0.6$ [21]. However,

transmission spectrum of the CIGS layer grown on the glass substrate was taken at normal incidence in an attempt to estimate the optical band gap E_g, hence to have a better accuracy for the value of x.

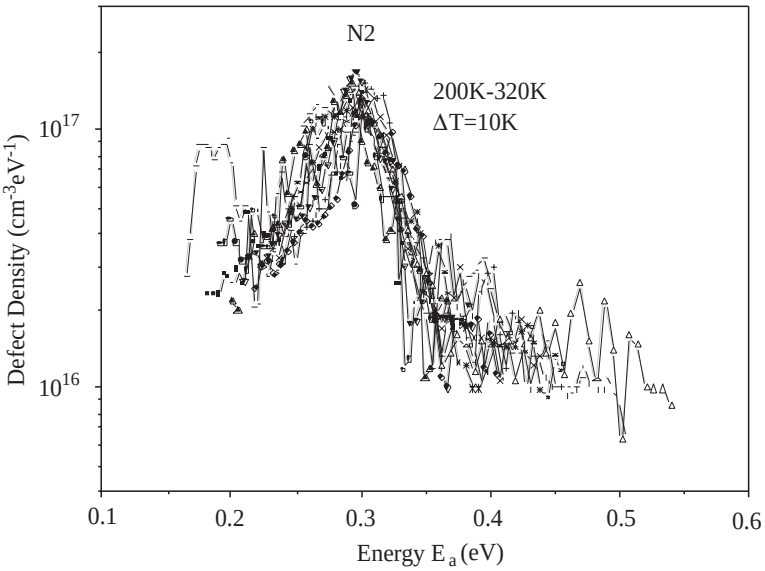

Figure 4. Defect spectra.

4.2. Determination of the optical band gap of Cu(In,Ga)Se_2 thin layers

Normal incidence optical transmission spectra of Cu(In,Ga)Se_2 layers grown on plain glass substrates were taken at room temperature in an attempt to estimate their optical band gap. Figure 5 shows the transmittance in the visible and near infrared range for a typical layer.

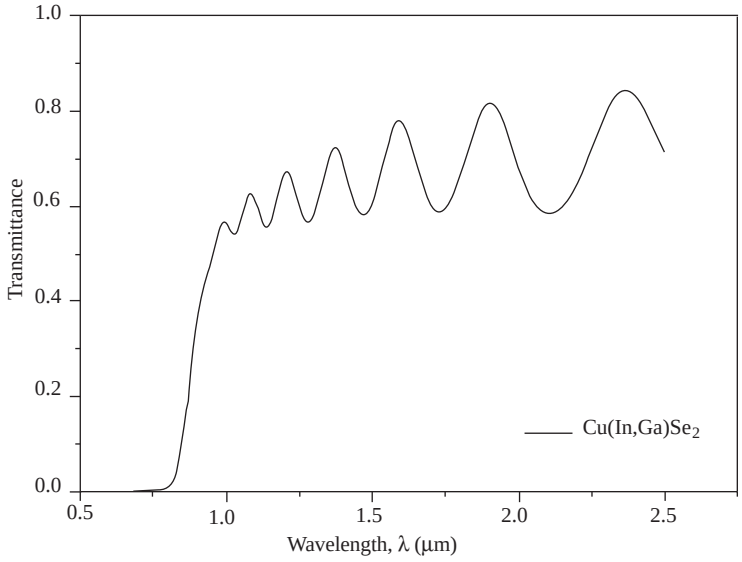

Figure 5. Normal incidence transmission spectra of the Cu(In,Ga)Se_2 layer.

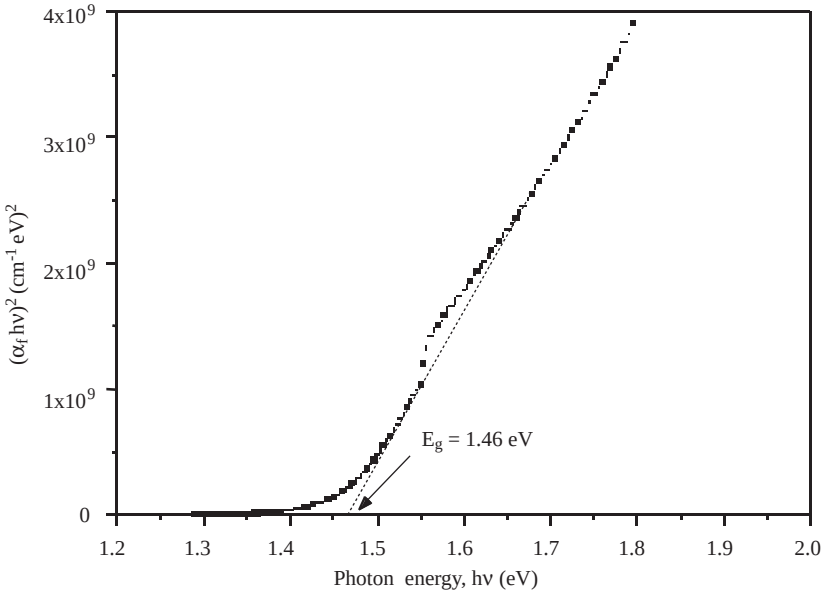

Figure 6. $(\alpha_f\, hv)^2$ vs. hv characteristics of the Cu(In,Ga)Se_2 layer.

Strong absorption was observed at wavelengths less than $0.94\,\mu\,m$ where the transmission virtually ceased. There was some residual absorption at long wavelengths giving rise to a reduction in the transmittance. However, this was more pronounced towards to the band edge probably due to the scattering, structural defects and excess carrier absorption. Following the procedure proposed by Swanepoel [22], α_f was calculated in the strong absorption region using extrapolated values of n_f. This was done by fitting Sellmeier functions of the form; $n_f^2 = a + b\,\lambda^2/\,(\lambda^2 - c^2\,)$ to values of n_f obtained in the weak absorption region. It is well-known that the increase in α_f at the band edge with photon energy $h\nu$ depends on the type of transition taking place and is given by the proportionality

$$\alpha \propto \frac{(h\nu - E_g)^{\xi}}{h\nu},$$

for allowed direct transitions, respectively (since Cu(In,Ga)Se_2 is a direct gap semiconductor, indirect transitions are not important), and E_g is the optical bandgap. Clearly, for allowed direct transitions, a plot of $(\alpha_f\, hv)^2$ vs. hv will give a straight line with an intercept on the axis equal to the band gap energy. A plot of $(\alpha_f\, hv)^2$ versus hv for Cu(In,Ga)Se_2 thin layer is shown in Figure 6. The linear straight line sections are clearly observed with an intercept on hv axis, corresponding to the values of 1.46 eV which corresponds to a Ga content x of about 0.7 [21].

5. Conclusion

AC admittance spectroscopy performed on n^+p rectifying junctions is a powerful technique to investigate the electrically active defects controlling the behavior of these devices. In the present work, a model initially developed for CIGS based devices has been applied to determine the bulk and interface defects in the absorber Cu(In,Ga)Se_2layer from temperature dependent capacitance spectra. The analysis of admittance data revealed the presence of a distribution of hole traps in the bulk or at the grain boundaries of the absorber layer, centered approximately at 300 meV with relatively high defect density of about 1.2×10^{17} eV^{-1} cm^{-3}. Accurate estimation for the value of x is provided by optical band gap determined by the procedure proposed by Swanepoel. The band gap of the absorber layer was found to be about 1.46 eV, which corresponds to a Ga content x of about 0.7, with x = Ga/(Ga+In).

Acknowledgements

The author is grateful to Prof. Dr. Şener Oktik, Dr. H. W. Schock U. Rau and all other colleagues in the IPE (Stuttgart University) for performing the fabrication of the heterojunction solar cell investigated in this work. The author also would like to thank Dr. Murat Bayhan for the transmission measurement.

References

[1] M. Contreras, B. Egaas, K. Ramanathan, J. Hiltner, A. Swartzlander, F. Hasoon, R. Nou, *Prog. Photovolt: Res. Appl.*, **7**, (1999), 311.

[2] U. Rau, H.W. Schock, *Cu(In,Ga)Se₂Solar Cells, in : M.D. Archer,* R. Hill (Eds.), Clean Electricity from Photovoltaics, Imperial College Press, London, UK, 2001.

[3] J.F. Guillemoles, *Thin Solid Films.*, **361–362**, (2000), 338.

[4] B. Dimmler, H.W. Schock, *Prog. Photovoltaics: Res. Appl.*, **6**, 81998), 193.

[5] A. Jasenek, U. Rau, *J. Appl. Phys.*, **90**, (2001), 650.

[6] A. Jasenek, U. Rau, V. Nadenau, D. Tiess and H. W. Schock, *Thin Solid Films.*, **361–361,** (2000), 415.

[7] U. Rau, M. Schmidt, A. Jasenek, G. Hanna and H. W. Schock*, Solar Energy Mat. And Sol. Cells.,* **67**, (2001), 137.

[8] M. Turcu and U. Rau, *Thin Solid films.*, **431–432**, (2003), 158.

[9] S. Siebentritt, *Thin Solid Films.*, **403–404,** (2002), 1.

[10] Q. Nyguen, K. Orgassa, I. Koetschau, u. Rau and H. W. Schock, *Thin Solid Films.*, **431–432,** (2003), 330.

[11] A. Jasenek, U. Rau, V. Nadenau, and H.W. Schock, *J. Appl. Phys.*, **87**, (2000), 594.

[12] J. Kneisel, K. Siemer, I. Luck and D. Bräunig, *J. Appl. Phys.*, **88**, (2000), 5474.

[13] R. Herberholz, M. Igalson, and H.W. Schock., *J. Apply. Phys.* **83,** (1998), 318.

[14] T. Walter, R. Herberholz, C. Muller and H.W. Schock., *J. Apply. Phys.* **80,** (1996), 4411.

[15] M. Igalson, and H. W. Schock., *J. Apply. Phys.* **80,** (1996), 5765.

[16] L. Stolt, K. Granath, E. Niemi, M. Bodegaerd, J. Hedstroem, S. Bocking, M. Carter, M. Burgelman, B. Dimmler, R. Menner, M. Powalla, U. Ruehle and H.W. Schock, Proc. 13^{th} European Photovoltaic Solar Energy Conference., (Nice, France) (1995) p 1451.

[17] J.D. Jackson, *Classical Electrodynamics,* 2^{nd} ed. (Wiley, New York, 1975), p. 311.

[18] K.W. Böer, *in Survey of Semiconductor Physics, Vol. I* (Van Nostrand Reinhold, New York, 1990), p.1135.

[19] Y. Zohta, *Solid –State Electron*, **16**, (1973), 1029.

[20] J.T. Healt, J.D. Cohen, W.N. Shafarman, D.X. Liao, and A.A. Rockett, *Appl. Phys. Let.,***80**, (2002),4540.

[21] G. Hanna, A. Jasenek, U. Rau, and H.W. Schock, *Thin Solid Films.*, **387**, (2001), 71.

[22] R. Swanepoel, *J. Phys. E. Sci. Instrum.*, **16,** (1985), 1214.